











# In situ and micro-Raman spectroscopy for the identification of natural Sicilian zeolites

Claudio Finocchiaro<sup>1</sup>  | Alessia Coccato<sup>1</sup>  | Germana Barone<sup>1</sup>  |  
Danilo Bersani<sup>2</sup>  | Adam Culka<sup>3</sup>  | Laura Fornasini<sup>4</sup>  |  
Paolo Mazzoleni<sup>1</sup>  | Jan Jehlička<sup>3</sup>  | Anastasia Rousaki<sup>5</sup>  |  
Peter Vandenabeele<sup>5,6</sup> 

<sup>1</sup>Department of Biological, Geological and Environmental Sciences, University of Catania, Catania, Italy

<sup>2</sup>Department of Mathematical, Physical and Computer Sciences, University of Parma, Parma, Italy

<sup>3</sup>Institute of Geochemistry, Mineralogy and Mineral Resources, Charles University, Prague, Czech Republic

<sup>4</sup>Institute of Chemistry of Organometallic Compounds, National Research Council (ICCOM-CNR), Pisa, Italy

<sup>5</sup>Department of Chemistry, Ghent University, Ghent, Belgium

<sup>6</sup>Department of Archaeology, Ghent University, Ghent, Belgium

## Correspondence

Alessia Coccato, Department of Biological, Geological and Environmental Sciences, University of Catania, Corso Italia, 57, 95127 Catania, Italy.  
Email: [alessia.coccato@unict.it](mailto:alessia.coccato@unict.it)

## Funding information

FWO-Vlaanderen, Grant/Award Number: 12X1919N; POFESR 2014-2020, Grant/Award Number: CUP G38I18000960007; Center for Geosphere Dynamics, Grant/Award Number: UNCE/SCI/006

## Abstract

Zeolites are present in numerous outcrops of volcanites of different ages in Sicily (Italy). Some of these outcrops are important because they constitute the ideal genesis conditions of some of these minerals, which represent geological indicators of chemical and geothermal gradients involved during their formation. For this purpose, a group of zeolites coming from areas of the Ionian coast and Palagonia village (Eastern Sicily) was investigated by means of Raman spectroscopy. In the geological record, these areas have been influenced by intense volcanic events that produced mineralization of hydrothermal origin. Sicilian zeolite samples were analysed in situ using different mobile Raman apparatus, directly on the outcrops of Aci Castello and the nearby Lachea Island, or in local collections where they are preserved. Some of these samples have been then analysed using laboratory micro-Raman to compare the results and identify the zeolite types. The strength and weakness points of each instrument have been highlighted. Often, the Raman spectra of zeolites are affected by broad fluorescence, making them of difficult interpretation. However, satisfying results were obtained with portable devices, whose identifications were confirmed by micro-Raman, discerning zeolites of different groups, such as analcime, chabazite, natrolite and phillipsite. The use of portable instruments has demonstrated the possibility to obtain identification of zeolites and related minerals both on site and in the laboratory, whose results match with the geological setting of the considered areas.

## KEYWORDS

in situ measurements, natural zeolites, portable Raman spectroscopy, Sicily, volcanism

This is an open access article under the terms of the [Creative Commons Attribution-NonCommercial-NoDerivs](https://creativecommons.org/licenses/by-nc-nd/4.0/) License, which permits use and distribution in any medium, provided the original work is properly cited, the use is non-commercial and no modifications or adaptations are made.

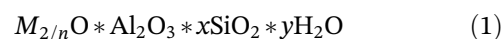
© 2021 The Authors. *Journal of Raman Spectroscopy* published by John Wiley & Sons Ltd.

## 1 | INTRODUCTION

The Sicilian geology is extremely complex and widely studied due to relevant tectonic events that affected the Mediterranean area.<sup>[1]</sup> The Eastern sector of the island displays interesting outcrops of volcanites combined with zeolite minerals, as a consequence of important volcanic events. In detail, the area close to Palagonia and Mineo villages, located in the Hyblean area, represents one of the earliest (200 to 1 My) volcanism manifestations, in submarine conditions, in the eastern part of the island, during the upper Pliocene, generating the Militello - Mount CalIELLA formation. This latter is characterized by the presence of palagonite, basaltic breccia, pillow lavas, hyaloclastites and zeolites that substitute the volcanic glass and fill in the vesicles (Figure 1a).<sup>[3-7]</sup> Next, the Ionic coast, extending from Aci Castello to Aci Trezza (Catania), represents the beginning of Etnean volcanism in submarine conditions, dated around 500 ky,<sup>[8]</sup> characterized by peperites (i.e., mixing of pillows lava and sediments) with zeolites inside<sup>[2]</sup> (Figure 1b).

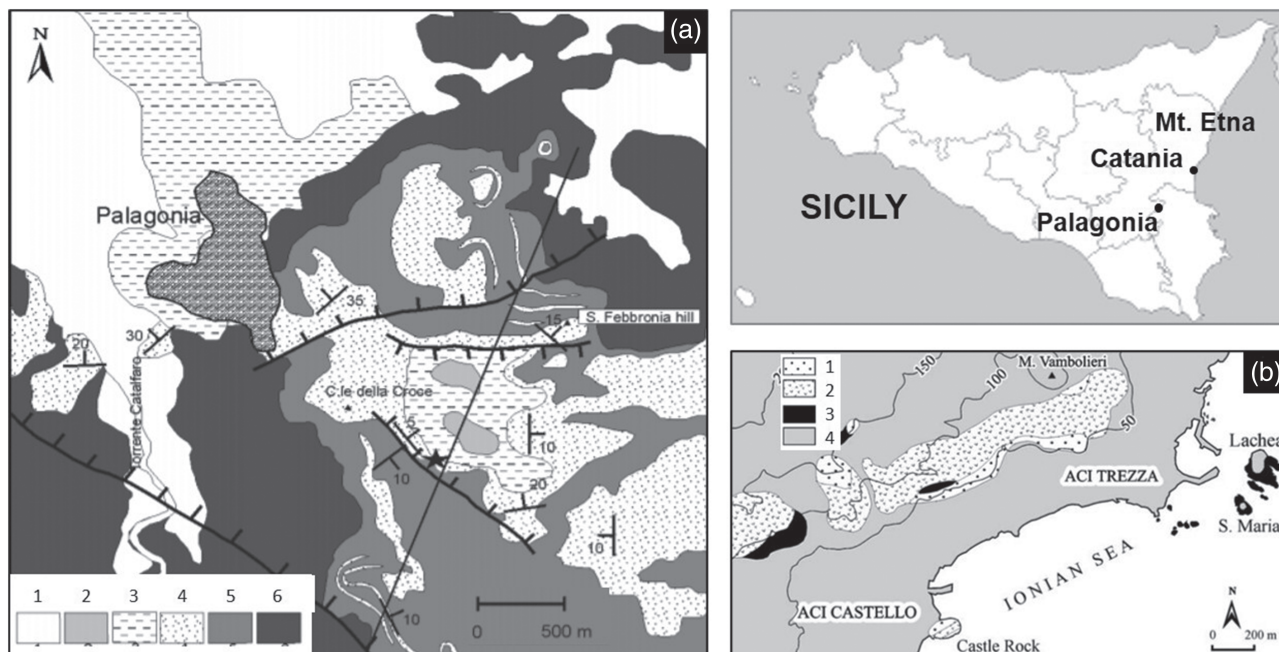
Zeolites, from ancient Greek meaning ‘boiling stones’,<sup>[9]</sup> are very interesting materials: natural ones inform us about geological events according to their geothermal or chemical gradient's information,<sup>[10,11]</sup> whereas on the other hand, they play an important role in industrial processes such as water purification,<sup>[12]</sup>

agriculture,<sup>[13]</sup> medicinal applications,<sup>[14]</sup> ion exchangers and molecular sieves<sup>[15]</sup> thanks to their chemical structure.<sup>[16]</sup> Moreover, they are used as precursors in alkaline activation process for the production of noncementitious binders (geopolymers<sup>[17-19]</sup>); they can also be present in pyroclastic materials used as raw materials for alkaline activation, as for example, Mount Etna ashes<sup>[20-23]</sup> or Lipari's pumices (Aeolian island-Sicily).<sup>[24]</sup> Zeolites have an aluminosilicatic framework based on an infinitely extending three-dimensional network of  $AlO_4$  and  $SiO_4$  tetrahedra linked to each other by sharing all oxygens, forming intracrystalline channels or interconnected voids, filled with water molecules and cations.<sup>[16,25-28]</sup> Chemically, zeolites are represented by the empirical formula shown in Equation 1.



where  $M$  is any alkaline cation,  $n$  represents the valence of the cation,  $x$  is the number of Si tetrahedra ( $2 \leq x < 10$ ) and  $y$  is the number of water molecules in the voids of the zeolite.<sup>[25]</sup>

Natural Sicilian zeolites are formed following abundant volcanic activity pre- and post-Mount Etna volcano formation, which has influenced their formation mainly through alteration phenomena of hydrothermal type.<sup>[16]</sup> This process is generated by the interaction of sea water



**FIGURE 1** Localization of outcropping areas with the corresponding geological maps: a) geology of Ionian east coast. Legend: 1) pillow lavas and pillow breccia; 2 = volcanoclastic deposits; 3 = subvolcanic rocks with columnar joints; 4 = alkaline volcanic and sedimentary rocks<sup>[2]</sup>; (b) geology of Palagonia area.<sup>[3]</sup> Legend: 1) recent and terrace alluvial deposits; 2) ‘Panchina’ (Middle Pleistocene); 3) Sandy claystone; 4) Emilian Calcarenes and sands; 5) Poggio Vina Formation; 6) Militello - Mount CalIELLA volcanism (Late Pliocene)

with lava ejected in submarine conditions,<sup>[29,30]</sup> modifying, after thousands of years, the volcanic glass in zeolite minerals. All zeolites are light coloured, of whitish, yellowish, bluish or pinkish shades. They occur in rocks as masses and, sometimes, especially in volcanic rocks, as crystalline aggregates. The zeolites outcropping in Sicily are listed in Table 1.

Typically, Sicilian zeolites belong to groups based on sodium exchangers cations: analcime,<sup>[2]</sup> chabazite-Na,<sup>[27]</sup> mesolite<sup>[31]</sup> and phillipsite-Na,<sup>[32]</sup> outcropping in the East coast of Catania between Aci Castello and Aci Trezza, whereas natrolite (or tetranatrolite) examples are found around Palagonia.<sup>[7,33]</sup> Generally, zeolites are composed of complex secondary building units based on four-, five- or six-membered rings of SiO<sub>4</sub><sup>4-</sup> and AlO<sub>4</sub><sup>5-</sup> tetrahedra.<sup>[34,35]</sup> They are often formed by hydrothermal interaction of tholeiitic, rhyolitic or alkali olivine basalts with alkali or alkali-earth containing solutions. The parent rock composition and porosity, and the hydrothermal solution's chemical composition, pH and temperature are the main parameters determining the type of zeolite. However, chemical, pH and temperature gradients may vary locally and through minerals crystallization, causing different paragenesis in the same environment<sup>[36,37]</sup> and across adjacent amygdales.<sup>[35,38–40]</sup> In this scenario, Gunter et al.<sup>[37]</sup> have observed natrolite fibres displaying a mesolite termination, whereas Triana et al.<sup>[36]</sup> report, in alkaline and tholeiitic basalts, the coexistence of natrolite with chabazite, of natrolite with analcime, as well as fan/radial aggregates of different varieties of fibrous zeolites (natrolite, mesolite & scolecite).

**TABLE 1** Chemical information on the main natural zeolites outcropping in Sicily according to [mindat.org](http://mindat.org)

Mineral name	General chemical formula
Analcime	Na (AlSi <sub>2</sub> O <sub>6</sub> ) · H <sub>2</sub> O
Chabazite-Na	(Na <sub>2</sub> ,K <sub>2</sub> ,Ca,Sr,Mg) <sub>2</sub> [Al <sub>2</sub> Si <sub>4</sub> O <sub>12</sub> ] <sub>2</sub> · 12H <sub>2</sub> O
Chabazite-K	(K <sub>2</sub> ,Ca,Na <sub>2</sub> ,Sr,Mg) <sub>2</sub> [Al <sub>2</sub> Si <sub>4</sub> O <sub>12</sub> ] <sub>2</sub> · 12H <sub>2</sub> O
Chabazite-Ca	(Ca,K <sub>2</sub> ,Na <sub>2</sub> ) <sub>2</sub> [Al <sub>2</sub> Si <sub>4</sub> O <sub>12</sub> ] <sub>2</sub> · 12H <sub>2</sub> O
Faujasite-Na	(Na <sub>2</sub> ,Ca,Mg) <sub>3.5</sub> [Al <sub>7</sub> Si <sub>17</sub> O <sub>48</sub> ] · 32H <sub>2</sub> O
Gismondine-Ca	CaAl <sub>2</sub> Si <sub>2</sub> O <sub>8</sub> · 4H <sub>2</sub> O
Gmelinite-Na	Na <sub>4</sub> (Si <sub>8</sub> Al <sub>4</sub> O <sub>24</sub> ) · 11H <sub>2</sub> O
Gmelinite-Ca	Ca <sub>2</sub> (Si <sub>8</sub> Al <sub>4</sub> O <sub>24</sub> ) · 11H <sub>2</sub> O
Gonnardite	(Na,Ca) <sub>2</sub> (Si,Al) <sub>5</sub> O <sub>10</sub> · 3H <sub>2</sub> O
Mesolite	Na <sub>2</sub> Ca <sub>2</sub> Si <sub>9</sub> Al <sub>6</sub> O <sub>30</sub> · 8H <sub>2</sub> O
Natrolite	Na <sub>2</sub> Al <sub>2</sub> Si <sub>3</sub> O <sub>10</sub> · 2H <sub>2</sub> O
Phillipsite-Na	(Na,K,Ca <sub>0.5</sub> ,Ba <sub>0.5</sub> ) <sub>4–7</sub> [Al <sub>4–7</sub> Si <sub>12–9</sub> O <sub>32</sub> ] · 12H <sub>2</sub> O
Phillipsite-Ca	(Ca <sub>0.5</sub> ,K,Na,Ba <sub>0.5</sub> ) <sub>4–7</sub> [Al <sub>4–7</sub> Si <sub>12–9</sub> O <sub>32</sub> ] · 12H <sub>2</sub> O

Even though these associations have been observed, the comprehension of the exact geochemical mechanisms is not trivial and not easily reproducible under laboratory conditions.<sup>[35,41]</sup> The crystallization order is well-known (chabazite, analcime, phillipsite & natrolite), as the initial formation of Na-zeolites followed by Ca-containing ones<sup>[35,37,41]</sup>; moreover, some indications have been reported on the petrogenetic conditions leading to specific paragenesis.<sup>[35]</sup> Nevertheless, as chemical variations and intergrowths have been observed at the microscopic scale by optical and electron microscopy, and chemically characterized by electron microprobe,<sup>[36,37]</sup> it appears that obtaining structural information with spatial resolution and chemical sensitivity is essential.

X-ray diffraction (XRD) is the classical technique for zeolites identification and discrimination.<sup>[42]</sup> Analyses are carried out under lab conditions and generally with powdered samples. More recently, non-destructive analytical tools, for example, Raman spectrometry are used in mineralogy, allowing to obtain vibrational spectroscopic data and identification of minerals either on very small specimens, particles or inclusions (commonly of micrometric dimension), and even outdoors. This has become possible thanks to the development of miniature instrumentation, which is being used in several scenarios and areas,<sup>[43–45]</sup> and appears to be more challenging.

Raman spectroscopy represents an advantageous and fast technique for the detection of minerals.<sup>[46]</sup> It has also been shown that this technique permits to identify and characterize organic minerals in the geological record. Nevertheless, zeolites were previously successfully investigated, and assignment of the Raman bands of common zeolites was carried out.<sup>[47–49]</sup> All the previous papers concerning Raman spectroscopy of zeolites report results obtained using Ar (514 nm), frequency-doubled Nd:YAG laser (532 nm) or exceptionally also 488 nm (Ar-ion laser).<sup>[48–50]</sup>

Generally, the Raman spectra of zeolites are affected by fluorescence, making them of difficult interpretation.<sup>[51]</sup> However, some studies on zeolites pointed out the usefulness, also, of portable Raman equipment aimed at overcoming the limitations of traditional autoptic observations of physical features (e.g. shape and colour), generally used for the identification of minerals in situ.<sup>[44,45,48–50]</sup> The previous experience using miniature instrumentation showed that near-infrared excitation was better to investigate a series of zeolites (thomsonite, stilbite, natrolite, eucalase & phenakite) compared to 532-nm excitation.<sup>[48–50]</sup> However, those investigations were carried out using a first generation portable Raman spectrometer with green excitation and the system generated measurement artefacts in several situations.

Generally, zeolites of the same group (e.g. natrolite-mesolite) have similar Raman spectra in the low-wavenumber range ( $100\text{--}1200\text{ cm}^{-1}$ ) and differ from each other in the OH-related vibrations. Therefore, these latter represent the most distinctive signals for a univocal identification. Complete spectra of zeolites in both spectral ranges are often lacking in literature data. In this work, Raman spectroscopy was applied to analyse Sicilian zeolites, directly on the outcrops of Aci Castello and the nearby Lachea Island through portable devices, as well as for the identification of zeolites belonging to a private collection with samples from Palagonia and Ionian coast. In this latter case, a micro-Raman spectrometer was also used. Moreover, portable devices were also used in laboratory conditions to compare the results with the corresponding analyses in situ. Therefore, the main aim of this work was to evidence in this geographical-geological context the strength and weakness points of each instrument used for the comparison of spectra obtained in different spectral ranges, measurement set-ups and measurement conditions. Moreover, the versatility of portable devices for field applications, also in non-ideal conditions and the potentiality to recognize very similar phases of zeolites belonging to the same subgroup, have to be underlined, with the aim to attract interest towards in situ Raman applications.

## 2 | MATERIALS AND METHODS

Different spot analyses were performed on the outcrops of Aci Castello and the nearby Lachea Island using two portable devices: a DeltaNu spectrometer (equipped with a 785-nm laser, maximum output power of 120 mW, wavenumber range of  $200\text{--}2000\text{ cm}^{-1}$ ) and an EnSpectr RaPort one (equipped with a 532-nm laser, maximum output power 30 mW, 0.5-mm spot size,  $100\text{--}4000\text{ cm}^{-1}$  spectral range with a spectral resolution of  $\sim 8\text{ cm}^{-1}$ ). Differently, some zeolites, coming from Palagonia and the Ionian coast (Aci Castello and Aci Trezza), belonging to a private collection were analysed with the same portable devices and with a Jasco NRS-3100 micro-Raman ( $50\times$  long working distance objective) with (1) a 532-nm source, approximately 8-mW laser power on the sample,  $0.5 \times 6\text{ mm}$  slit, 10 accumulations of 120 s each and (2) a 785-nm source, approximately 10-mW laser power on the sample,  $0.5 \times 6\text{ mm}$  slit, 20–40 accumulations of 30–60 s each. For portable instruments, no calibration is required before measurements, although it has been checked with reference standard materials; differently, for the laboratory, one this was done using the  $520.7\text{ cm}^{-1}$  Raman band of silicon before each experimental session. However, only portable devices could be used for sample

zeo 5 due to its considerable size, unsuitable for the micro-Raman instrument.

The in situ measurements were particularly challenging as geometrical constraints and direct sunlight/shadow had to be taken into account. Moreover, different laser wavelengths and combinations of time, accumulations and laser power were tested by performing quick measurements ( $<25\text{ s}$ ): On the basis of these quick tests, evaluated directly on site, the acquisition conditions were optimized and only the best spectra (in terms of signal-to-noise ratio [SNR]) were kept. The Raman signals were then collected with longer acquisition times both in the low-wavenumber range (T–O–T bending and stretching vibrations) and in the OH stretching region. Samples were also acquired covering the observed variability of zeolite minerals for testing under laboratory conditions. Table 2 lists information on collection's zeolites together with their pictures, whereas most of the analysed crystals during in situ analyses are transparent trapezohedra embedded in the dark volcanic rock. Other sampled minerals occurring in small geodes showed the aspect of clusters of whitish prismatic crystals or spherical aggregates of needle-like crystals.

The zeolites of the collection were selected according to the presence of different crystalline aggregates, taking into account their shape and dimensions to avoid any damage to the specimens during the measurements (Table 2).

Baseline correction was performed with *LabSpec* software. Spectra of the aluminosilicatic vibrations region (below  $1200\text{ cm}^{-1}$ ) are given for all samples. The OH vibrations range ( $3000\text{--}3700\text{ cm}^{-1}$ ) were obtained from the RaPort and Jasco instruments with 532-nm lasers.

The Raman identification of zeolitic phases was performed through comparison with literature data.<sup>[34,48,52]</sup>

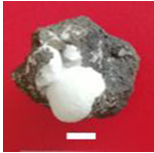



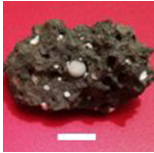
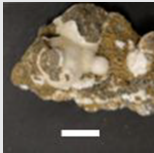
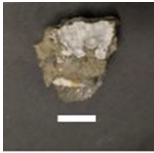
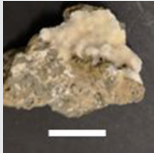
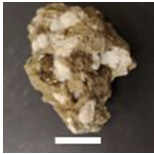
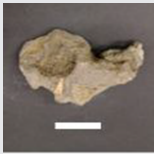
## 3 | RESULTS AND DISCUSSION

Representative spectra obtained with all the different instruments are reported in the low-wavenumber range ( $200\text{--}1200\text{ cm}^{-1}$ ) in Figures 2–7, S1, S3, S4 and S5, whereas for the ones obtained with the green laser, also the OH-vibration range is given ( $3000\text{--}3700\text{ cm}^{-1}$ ) in Figures 2, 4, 7 and S2. Moreover, band positions are reported in Table 3.

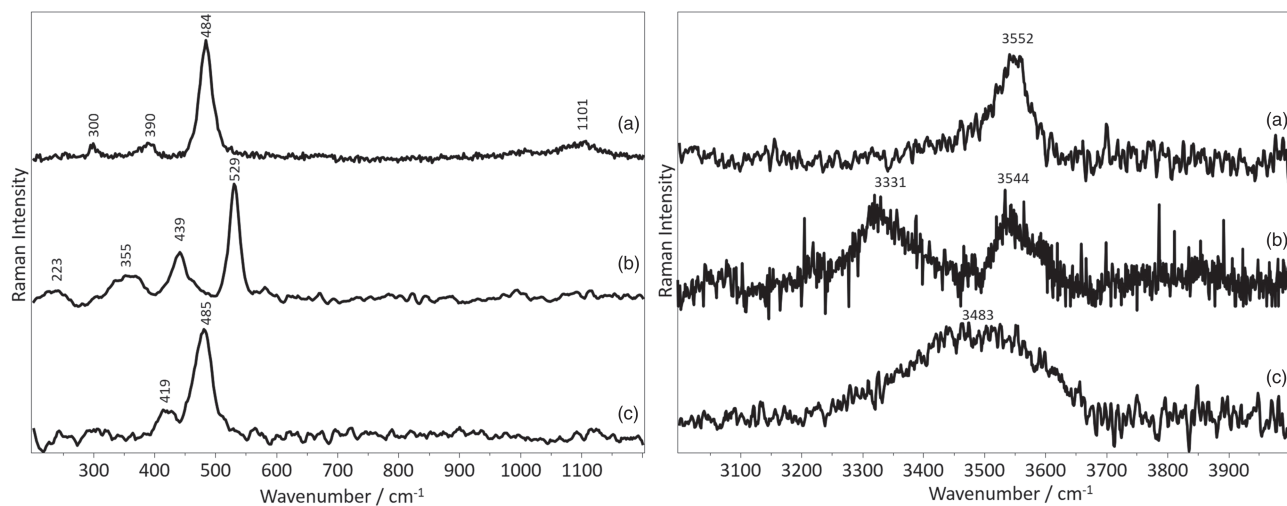
### 3.1 | In situ measurements

At different locations, different spectra were obtained. Raman spectra acquired with RaPort instrument on Lachea island show bands at approximately 300, 390 and

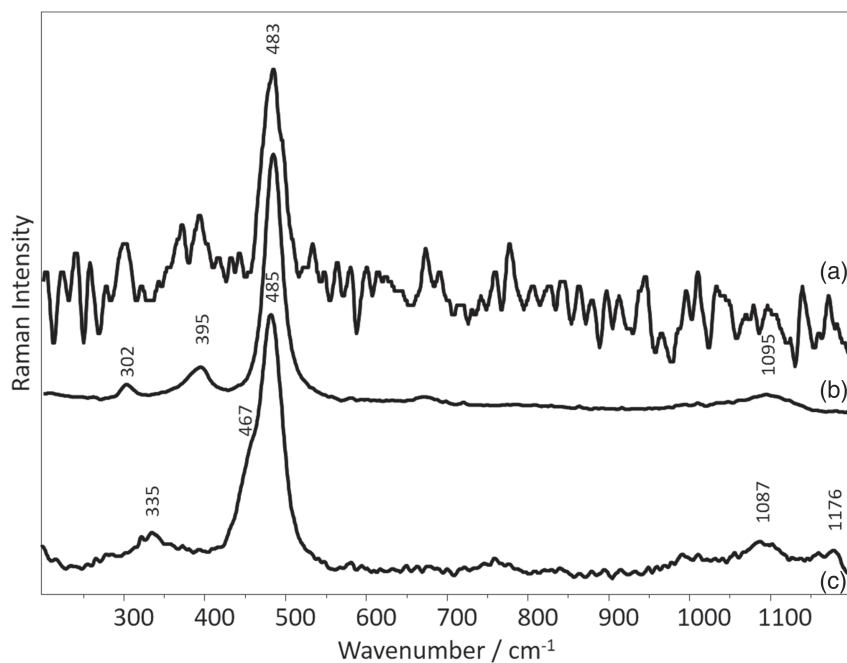
**TABLE 2** Main information and macroscopic observation of zeolites analysed

Sample	Locality	Description	
Zeo 1	Palagonia	White hemispherical structures made of thin needle-like prismatic crystals	
Zeo 2	Aci Castello	Irregular clusters of transparent/whitish crystals	
Zeo 4	Palagonia	Large opaque white surface	
Zeo 5	Aci Trezza	Transparent crystals (crystal aggregate)	
Zeo 6	Palagonia	Small white spherical structures	
Zeo 8	Palagonia	White hemispherical structures made of thin needle-like prismatic crystals	
Zeo 9	Palagonia	Small white spherical structures with granular shape	
Zeo 16	Aci Castello	White structures made of thin needle-like prismatic crystals	
Zeo 16 new	Aci Castello	White and transparent structures with granular shape	
Analcime	Aci Castello	Transparent and dark crystals (crystal aggregate)	

Note: In each picture, the white scale bar is 1 cm.



**FIGURE 2** Spectra collected with RaPort (532 nm) device in outdoor conditions on locations of the Ionian coast. Legend: analcime (a); natrolite (b); phillipsite (c)

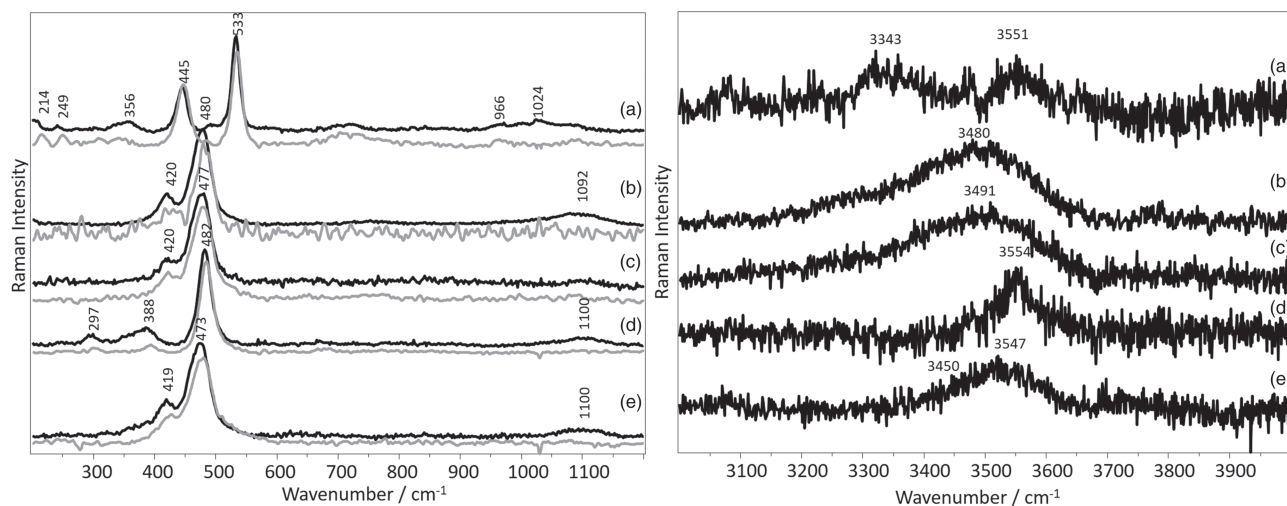


**FIGURE 3** Spectra collected with DeltaNu (785 nm) device on: analcime sample in outdoor (a) and in laboratory (b) conditions; spectrum of chabazite sample (c) in laboratory conditions

484  $\text{cm}^{-1}$  (Figure 2, spectrum a), moreover, in the green laser excited spectrum a broad band centred at 1101  $\text{cm}^{-1}$  is also visible (Figure 2, spectrum a). These bands (Table 3), compared with literature,<sup>[34]</sup> correspond to analcime Raman signals. On Lachea island, the low-wavenumber region also allowed the identification of natrolite (Figure 2, spectrum b, 223, 355, 439 and 529  $\text{cm}^{-1}$ ) and of phillipsite (Figure 2, spectrum c, 419 and 485  $\text{cm}^{-1}$ ). The OH-spectra shown in Figure 2, obtained on site with the RaPort instrument, show different Raman signatures, confirming the identification obtained from the low-wavenumber region: Analcime has a relatively sharp band (ca. 200  $\text{cm}^{-1}$  at the baseline)

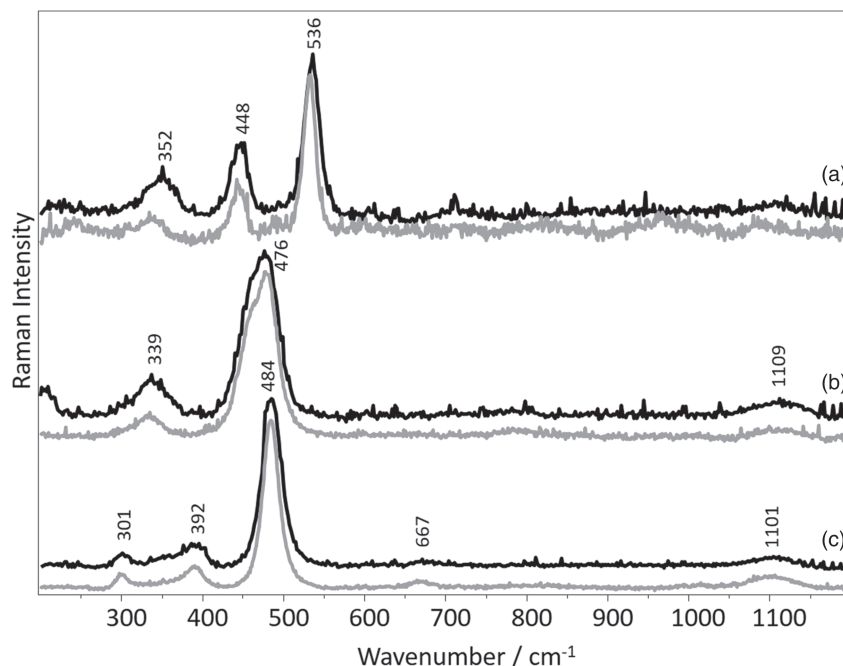
at approximately 3550  $\text{cm}^{-1}$  (Figure 2, spectrum a), natrolite has two bands centred at approximately 3330 and 3540  $\text{cm}^{-1}$  (ca. 250 and 200  $\text{cm}^{-1}$  at the baseline, respectively) (Figure 2, spectrum b), phillipsite a very broad band (ca. 500  $\text{cm}^{-1}$  at the baseline) at approximately 3480  $\text{cm}^{-1}$  (Figure 2, spectrum c).

The spectra obtained with DeltaNu instrument on site and in the laboratory on samples from Lachea and Aci Trezza boulders are shown in Figure 3. The identification of analcime (Figure 3, spectra a and b; Table 3) has been possible both on site and in less severe conditions inside the laboratory, respectively, thanks to the main band at 485  $\text{cm}^{-1}$  and to the weaker signals at 302, 395 and



**FIGURE 4** Spectra collected with RaPort (532 nm; black) and DeltaNu (785 nm; grey) devices in the 200–1200  $\text{cm}^{-1}$  range. Spectra collected with RaPort device are also shown for the OH range. Legend: Zeo 1 (a); Zeo 2 (b); Zeo 4 (c); Zeo 5 (d); Zeo 6 (e)

**FIGURE 5** Spectra collected with micro-Raman Jasco device with two different laser sources: 785 nm (black) and 532 nm (grey). Legend: Zeo 1 (a); Zeo 9 (b); analcime from Lachea island (c)



1095  $\text{cm}^{-1}$ , only visible in the better quality spectrum (Figure 3, spectrum b). In the latter case, the SNR is greatly improved. Moreover, a sample taken to the lab (Figure 3, spectrum c; Table 3) allowed the identification of chabazite thanks to the bands at 335, 483 (with a shoulder at 467), 1087 and 1176  $\text{cm}^{-1}$ .

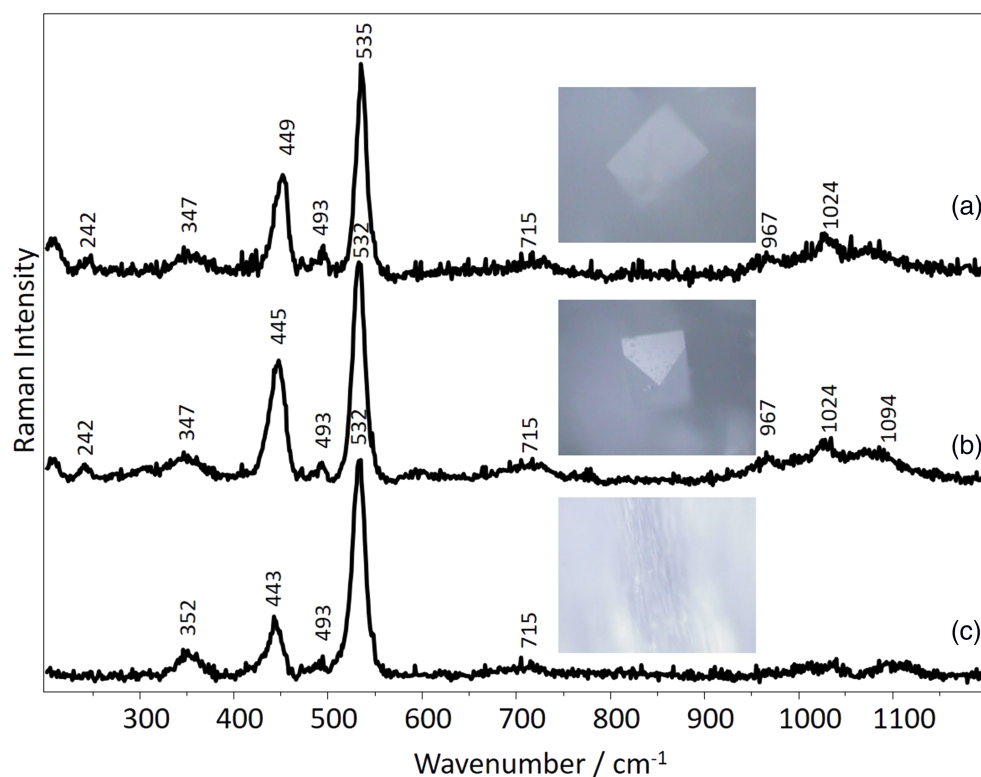
### 3.2 | Private collection samples

For the zeolite samples of the private collection, both portable and laboratory instrumentation could be used, except for Zeo 5 that was too big for the microscope stage.

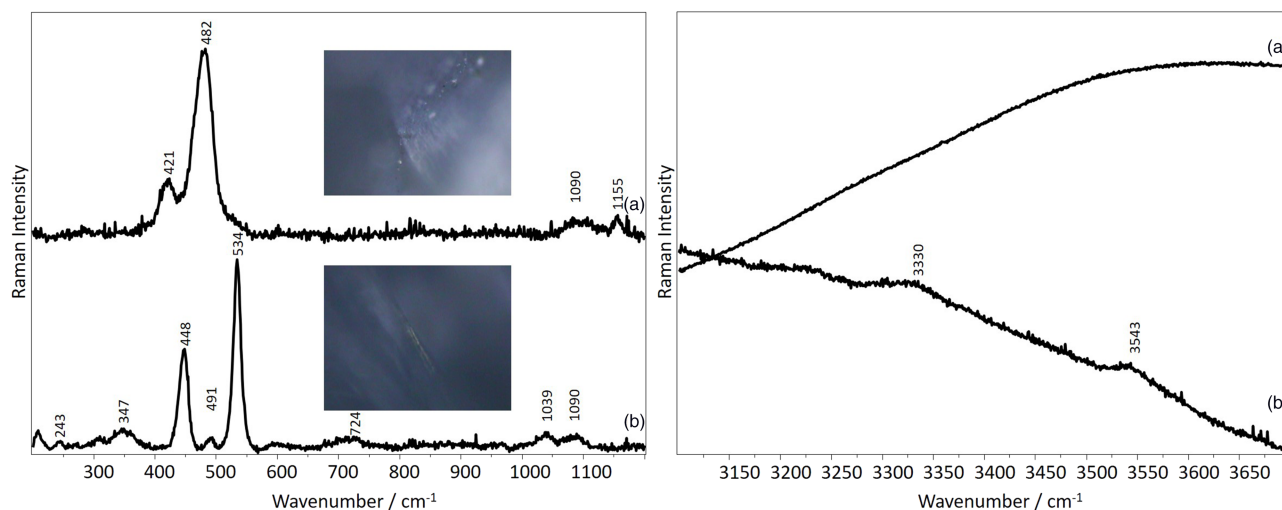
The acquired spectra are reported in Figure 4 for the low-wavenumber region with both portable devices and for the OH region with RaPort, and in Figures 5, 6 and 7 with the micro-Raman spectrometer. The Raman band positions are reported in Table 3.

### 3.3 | Portable instruments

Figure 4 reports representative spectra acquired on the private collection samples with the two different portable instruments used in laboratory conditions. Sample Zeo 1 (Figure 4, spectra a) is identified as a member of the



**FIGURE 6** Spectra acquired on Zeo 8 sample in the 200–1200  $\text{cm}^{-1}$  range by means of micro-Raman Jasco device (532 nm). Legend: I spot analysis (a); II spot analysis (b); III spot analysis (c)



**FIGURE 7** Spectra collected in 200–1200 and 3000–3700  $\text{cm}^{-1}$  range with micro-Raman Jasco device (532 nm). Legend: Zeo 16 new (a); Zeo 16 (b)

natrolite group based on the bands at 356, 445, 533, 1024, 3343 and 3551  $\text{cm}^{-1}$ . Sample Zeo 2 (Figure 4, spectra b), with bands at 420, 480, 1092 and 3480  $\text{cm}^{-1}$  is identified as phillipsite. The same identification applies to sample Zeo 4 (Figure 4, spectra c). Sample Zeo 5 (Figure 4, spectra d), with bands at 297, 388, 482, 1100 and 3554  $\text{cm}^{-1}$  is interpreted as analcime. Finally, also sample Zeo 6 (Figure 4, spectra e) is interpreted as phillipsite showing bands at 419, 473, 3450 and 3547  $\text{cm}^{-1}$ .

### 3.4 | Micro-Raman instrument

Figure 5 shows spectra acquired on the private collection samples with the micro-Raman instrument using both lasers. The low-wavenumber spectra acquired on sample Zeo 1 (Figure 5, spectra a) are given for comparison with the spectra obtained with the portable devices (Figure 4, spectra a): The band positions are generally in good agreement (Table 3) and confirm the capability of both



TABLE 3 Raman band positions for the spectra presented

Spectrum name	Wavelength (in nm), portable instrument in situ/in lab or fixed instrument	Spectrum in figure	Band positions (in cm <sup>-1</sup> )
Analcime	532 portable in situ	Figure 2a	300 390 484
Natrolite	532 portable in situ	Figure 2b	223 355 439 529
Phillipsite	532 portable in situ	Figure 2c	419 485
Analcime	785 portable in situ	Figure 3a	483
Analcime	785 portable in lab	Figure 3b	302 395 485
Chabazite	785 portable in lab	Figure 3c	335 467 485
Zeo 1	785 portable in lab	Figure 4a	214 249 445 533
Zeo 1	532 portable in lab	Figure 4a	242 356 445 533
Zeo 2	785 portable in lab	Figure 4b	420 480
Zeo 2	532 portable in lab	Figure 4b	420 480
Zeo 4 bluish	785 portable in lab	Figure 4c	420 477
Zeo 4 bluish	532 portable in lab	Figure 4c	420 477
Zeo 5	785 portable in lab	Figure 4d	300 393 484
Zeo 5	532 portable in lab	Figure 4d	297 388 482
Zeo 6 bluish	785 portable in lab	Figure 4e	419 473
Zeo 6 bluish	532 portable in lab	Figure 4e	419 473
Zeo 1	532 fixed	Figure 5a	352 536
Zeo 1	785 fixed	Figure 5a	352 448 536
Zeo 9	532 fixed	Figure 5b	339 476
Zeo 9	785 fixed	Figure 5b	339 476
Analcime	532 fixed	Figure 5c	301 392 484
Analcime	785 fixed	Figure 5c	301 392 484
Zeo 8	532 fixed	Figure 6a	242 347 449 493 535
		Figure 6b	242 347 445 493 532
		Figure 6c	352 443 493 532
Zeo 16_new	532 fixed	Figure 7a	243 347 491 448 534
Zeo 16	532 fixed	Figure 7b	421 482
Natrolite (Vicenza, Italy)	532 portable in lab	Figures S1–S2	160 303 332 355 441 530
Mesolite (Iceland)	532 portable in lab	Figure S1	292 420 446 533
Scolecite (India)	532 portable in lab	Figures S1–S2	153 183 435 447 535

TABLE 3 (Continued)

<b>Spectrum name</b>	<b>Wavelength (in nm), portable instrument in situ/in lab or fixed instrument</b>	<b>Spectrum in figure</b>	<b>Band positions (in cm<sup>-1</sup>)</b>
Natrolite (Tyrol, Italy)	785 portable in lab	Figures S3 & S5	307 360 441
Natrolite (Tyrol, Italy)	532 fixed	Figure S3	307 332 358 441 532
Natrolite (Tyrol, Italy)	785 fixed	Figure S3	444 536
Mesolite (Iceland)	785 portable in lab	Figure S4	417 444 531
Mesolite (Iceland)	532 fixed	Figure S4	423 446 533
Mesolite (Iceland)	785 fixed	Figure S4	426 449 535

Note: Band positions in bold are the most intense ones.

TABLE 3 (Continued)

<b>Spectrum name</b>	<b>Band positions (in cm<sup>-1</sup>)</b>
Analcime	1001 3552
Natrolite	3331 3544
Phillipsite	3483
Analcime	
Analcime	1095
Chabazite	1087 1176
Zeo 1	966 1024
Zeo 1	1024 3343 3551
Zeo 2	
Zeo 2	1092 3480
Zeo 4 bluish	
Zeo 4 bluish	3491
Zeo 5	
Zeo 5	1100 3473 3554
Zeo 6 bluish	
Zeo 6 bluish	1100 3450 3547
Zeo 1	
Zeo 1	
Zeo 9	1109
Zeo 9	1109

TABLE 3 (Continued)

Spectrum name	Band positions (in cm <sup>-1</sup> )									
Analcime	667								1101	
Analcime	667							1101		
Zeo 8	715		967	1024						
	715		967	1024						
	715									
Zeo 16_new	724			1039	1090	1090	3233	3330		3543
Zeo 16					1090		1155			
Natrolite (Vicenza, Italy)	703	727	962	1035	1084			3326		3533
Mesolite (Iceland)	711	757		1042			3240		3400	3530
Scolecite (India)				1045	1098		3236	3322	3413	3503
Natrolite (Tyrol, Italy)	703	727		1037						3578
Natrolite (Tyrol, Italy)	704	726	965	1037	1089					
Natrolite (Tyrol, Italy)			956	1041						
Mesolite (Iceland)	711	753		1041						
Mesolite (Iceland)	714			1042						
Mesolite (Iceland)				1045						

Note: Band positions in bold are the most intense ones.

lasers of identifying zeolites of the natrolite group. Moreover, this identification can be easily obtained with both a portable or laboratory instrument. Sample Zeo 9 (Figure 5, spectra b) shows bands at 339, 476 (with a shoulder at ca. 460  $\text{cm}^{-1}$ ) and a broad and weak feature at 1109  $\text{cm}^{-1}$ , visible with both lasers. This spectrum is typical of chabazite. Finally, a sample from Lachea island (Figure 5, spectra c) shows once again the signature of analcime with bands at 301, 392, 484, 667 and 1101  $\text{cm}^{-1}$ .

The three low-wavenumber spectra acquired on sample Zeo 8 with the 532-nm laser (Figure 6) are worthy of consideration, as they are all compatible with a natrolite-group identification with the main band at approximately 530  $\text{cm}^{-1}$ . Nevertheless, they display variable band positions in the 440–450, 530–535 and 1000–1100  $\text{cm}^{-1}$  regions. The observed shift between spectra a and b of Figure 6 is not due to calibration issues, but it is most likely associated with the chemical variability of natural zeolites at the microscopic scale.<sup>[35,38–41,53]</sup> On the other hand, the variation in relative intensities of the bands, observed between spectra b and c of Figure 6, could be due to orientational effects, which are well known for zeolites.<sup>[48]</sup> Specifically, spectrum b was obtained on the terminal facets of a fibre and spectrum c perpendicularly to the fibre itself, as shown in the microphotographs in Figure 6. These observations could only be made on spectra obtained with the micro-Raman spectrometer, as an accurate control of the sample morphology can be easily achieved, and the spectra could therefore be linked to chemical zoning or to symmetry-related effects, especially in fibrous zeolites.

Concerning the chemical variability of zeolites, it appears that different minerals are formed according to the local conditions, and the same sample could yield completely different Raman signatures, as shown by sample Zeo 16, Figure 7. The euhedral crystal (spectrum a) is a phillipsite (421, 482 & 1155  $\text{cm}^{-1}$ ), even though the high wavenumber range shows an intense fluorescence, whereas the fibrous one (243, 347, 448, 491, 534, 724, 1039, 1090, ca. 3330 and ca. 3540  $\text{cm}^{-1}$ ) corresponds to a natrolite composition.

Moreover, in order to further test portable and laboratory instruments, different zeolites belonging to the same subgroup have been distinguished and identified. Raman spectra acquired on three different zeolites of the natrolite subgroup are shown in Figures S1–S5. Natrolite, mesolite and scolecite have been identified.<sup>[48,54,55]</sup>

The identification has been made both in the low-wavenumber spectral range and in the OH stretching vibration region. In the first one, the distinction of different zeolites has been achieved using portable and laboratory instruments. Raman spectra are in good agreement

and peak positions occur within few wavenumbers (band positions are reported in Table 3). In addition, the OH stretching vibration modes, collected with the RaPort spectrometer, confirm the identification of the three zeolites, which show characteristic OH signals.

The observed band positions were compared with literature: It appears that the main band position, either around 480 or 530  $\text{cm}^{-1}$ , is indicative of the secondary building units, as it is assigned to T–O–T bending vibrations. In the first case, it indicates zeolites based on single four-membered rings such as analcime and phillipsite,<sup>[34]</sup> whereas in the second, it is typical of zeolites based on connected four-membered rings (natrolite group).<sup>[34,48]</sup> Chabazite, with its double six-membered rings structure has a lower band position with respect to single four-membered rings zeolites.<sup>[34]</sup> As already reported in literature, the discrimination among the different zeolites cannot be performed solely on the main Raman band, and the presence of mineral aggregates and of chemical zoning in the same crystal have been highlighted.<sup>[34,36,37,48]</sup> In particular, it appears that the natrolite group is problematic as it concerns autoptic and bulk identification, so care has to be taken in this respect, as it seems that the OH region is definitely more diagnostic than the low-wavenumber region.

As seen from Figure 4, the achieved full-width at half maximum (FWHM) of both mobile spectrometers is highly similar. In addition, the FWHM values obtained with portable instruments are comparable with those of the laboratory equipment. Differences in width are expected for crystals with narrow signals when instruments with different spectral resolution are used. However, it does not appear that the FWHM of Raman peaks is significantly affected by the instrumental broadening, when using portable devices on zeolites. The SNR of the DeltaNu spectrometer seems to be slightly worse than the one of the RaPort spectrometer but still comparable with laboratory Raman spectrometers. SNR ratios are determined by experimental (outdoor) conditions, detector sensitivity as a function of the laser wavelength and the spectrometer optics that are involved. Moreover, signal intensity is determined by the Raman sensitivity and orientation of the mineral at hand.

### 3.5 | Portable Raman spectrometers versus traditional techniques

Notoriously, the most used technique for zeolites identification is XRD.<sup>[42]</sup> This requires the sample being powdered,<sup>[56]</sup> or an accurate preparation for single-crystal set up.<sup>[57]</sup> The identification of zeolites of the same subgroup (e.g. natrolite-mesolite) is often difficult because

the patterns are very similar, due to the correspondence of the main peaks.

Differently, Raman spectroscopy carried out with portable devices, ranging up to  $3700\text{ cm}^{-1}$  (as with RaPort), allows to detect the OH vibrations, able to univocally identify zeolites species also of the same subgroup (supporting information). This important advantage is added to the possibility to carry out systematic in situ campaigns with robust devices, easy to transport and to handle, allowing to characterize numerous outcroppings and, based on those observations, to perform a strategic sampling campaign for further laboratory tests.

One of the main advantages of in situ measurements with portable spectrometers is the relatively short time for individual analysis. Obviously, the longer the acquisition times and the higher number of accumulations, the better the final Raman spectra will be. This is true both for the analyses using portable and laboratory spectrometers. However, in situ or even in the field measurement approach often asks for the 'optimized' settings, which typically means short total time for a single analysis. This optimization is largely instrument-dependent, as the differences among the portable or handheld spectrometers are substantial. In this study, the  $<25\text{ s}$  settings for one in situ analysis of zeolite provided good quality data (unambiguous identification) when the RaPort spectrometer ( $532\text{ nm}$ ) was used (Figure 2). The DeltaNu spectrometer ( $785\text{ nm}$ ) on the other hand would benefit from longer times for each analysis, since as illustrated in Figure S5, the noise levels are substantial for short analyses times. The minimum setting of 5 acquisitions of 5 s each for single analysis typically provided workable quality of data with respect to identification. However, the spectrum taken at 10 acquisitions of 10 s each featured a significantly better band resolution (Figure S5) mainly for the important Raman bands below  $500\text{ cm}^{-1}$ . The total time for individual analysis in this case is still under 2 min ( $100\text{ s}$ ), which is considerably longer than 25 s, but still within a reasonable timeframe. A possible explanation of this significant difference in the quality of Raman spectra acquired with the two instruments might be that the  $532\text{-nm}$  excitation is more efficient than the  $785\text{ nm}$  for this kind of mineralogical samples. Another possible factor is that the RaPort spectrometer is more than 10 years 'younger' than DeltaNu and, in this time, the technology and consequent usability with respect to miniaturized Raman spectrometers in geoscience has seen major advances.<sup>[58]</sup>

## 4 | CONCLUSIONS

As the characterization performed on site as well as on collectors' samples demonstrated, Raman spectroscopy is

a powerful tool for discriminating among different zeolites<sup>[34,48,51,59,60]</sup>; the potentiality of in situ identification of the exact structure is paramount for geological applications.<sup>[44,45]</sup>

It appears that the most diagnostic Raman bands are the ones at approximately  $400\text{--}500\text{ cm}^{-1}$ , assigned to ring structures present in the framework,<sup>[60]</sup> specifically to T—O—T (T=Al or Si) bending vibration.<sup>[48,50]</sup> The OH region is also indicative, as well known also for other hydrated minerals.<sup>[61]</sup>

From the geological point of view, the identification of zeolitic minerals, corresponding to a well-known alteration of volcanites in hydrothermal conditions, allows to have an idea on the chemistry of the hydrothermal fluid, which seems to be rich in sodium for the zeolite species identified. This consideration agrees with the underwater genesis of areas considered. Therefore, they represent useful geological indicators.<sup>[10,11]</sup> The identification results are in good agreement with the geology of the outcrops. Indeed, according to literature data, the zeolites sampled at Mount Calielia (Palagonia) belong, mainly, to natrolite family,<sup>[7]</sup> whereas the zeolites of the Ionic coast are reported to be analcime and phillipsite.<sup>[2]</sup> As the discrimination between natrolite and mesolite is hampered by their similarity, which is reflected also in their Raman spectra, the identification of natrolite for the first time by in situ measurements on the East coast of Sicily is mainly based on the OH region. The lack of consistent reference spectra as well as of detailed compositional characterization should be taken into account when zeolites are characterized by Raman spectroscopy.

For the sake of species identification, portable spectrometers results are in agreement with those of laboratory instruments, preserving the advantages of the in situ work. Through that, the minerals can be studied directly in their environment, in relation with other minerals and rocks. This can support the sampling campaign, limiting the risks of an incomplete or non-adequate material collection.

The comparison between in situ and laboratory analyses with portable spectrometers confirms that the identification of the zeolites can be obtained in the field. In addition, further details can be obtained with laboratory investigations. For example, the number of peaks detected with portable instruments in the lab is even comparable with that obtained with laboratory spectrometers, except for few missing signals that cannot be resolved in weak doublets or triplets of very close-lying peaks.

Furthermore, working with portable spectrometers with extended spectral range including the OH stretching region (until  $3700\text{ cm}^{-1}$ ) makes the distinction among different phases easier, also during on site campaigns. It is well known that in the low-wavenumber range (under

1200 cm<sup>-1</sup>), the Raman features of zeolites in terms of differences in the peak positions or band intensities can be clearly distinguished only in pure end-members or in ideal working conditions. On the other hand, the OH stretching signals are a sensitive probe for the distinction of slight variations in the structure or in the composition. Therefore, despite the spectral resolution of portable devices being lower than that of laboratory instruments, the distinction among different zeolites has been easily obtained in situ through analyses with portable spectrometers that can detect OH stretching vibrations, as demonstrated by the RaPort measurements. Moreover, as the extended-range spectra of zeolites are not systematically published, the data here reported are filling the existing gap in the framework of natural Sicilian zeolites.

In summary, the results of the in situ analyses with portable Raman instruments can be used to support further research for the study of minerals in extreme outdoor conditions.


## ACKNOWLEDGEMENTS

This research is supported by the found of POFESR 2014-2020 project entitled 'Sicilia Eco Innovative Technologies - SETI', CUP G38I18000960007. A. Rousaki wishes to acknowledge FWO-Vlaanderen for her post-doctoral grant (project 12X1919N). The authors want to thank Mr Franco Belluso to have kindly allowed the analysis of some zeolites of his private collection. A. Culka and J. Jehlička were partly supported by institutional funding from the Center for Geosphere Dynamics (UNCE/SCI/006). Open Access Funding provided by Università degli Studi di Catania within the CRUI-CARE Agreement.

## ORCID

Claudio Finocchiaro  <https://orcid.org/0000-0002-8841-283X>

Alessia Coccato  <https://orcid.org/0000-0002-6641-2820>

Germana Barone  <https://orcid.org/0000-0003-0822-2436>


Danilo Bersani  <https://orcid.org/0000-0002-8026-983X>

Adam Culka  <https://orcid.org/0000-0002-1861-070X>

Laura Fornasini  <https://orcid.org/0000-0002-6794-0828>

Paolo Mazzoleni  <https://orcid.org/0000-0002-7281-923X>

Jan Jehlička  <https://orcid.org/0000-0002-4294-876X>

Anastasia Rousaki  <https://orcid.org/0000-0002-4302-7276>

Peter Vandenabeele  <https://orcid.org/0000-0001-5285-9835>

## REFERENCES

- [1] L. Basilone, *Lithostratigraphy of Sicily*, Assessorato del Territorio e dell'Ambiente Regione Siciliana, Palermo **2012**.
- [2] R. A. Corsaro, P. Mazzoleni, J. Volcanol, *Geotherm. Res.* **2002**, *114*, 219. [https://doi.org/10.1016/S0377-0273\(01\)00290-6](https://doi.org/10.1016/S0377-0273(01)00290-6)
- [3] R. Punturo, G. Sturiale, C. Vaccaro, R. Cirrincione, A. Mustica, *Ital. J. Geosci.* **2013**, *132*, 263.
- [4] H.-U. Schmincke, B. Behncke, M. Grasso, S. Raffi, *Geol. Rundsch.* **1997**, *86*, 637.
- [5] N. A. Stroncik, H. U. Schmincke, *Int. J. Earth Sci.* **2002**, *91*, 680.
- [6] Y. V. Frolova, *Moscow Univ. Geol. Bull.* **2010**, *65*, 104.
- [7] G. Sicurella, S. Russo, E. M. Ciriotti, G. Blass, *Micro (località)* **2010**, *2*, 371.
- [8] P. Y. Gillot, G. Kieffer, R. Romano, *Acta Vulcanol.* **1994**, *5*, 81.
- [9] D. S. Coombs, A. Alberti, T. Armbruster, G. Artioli, C. Colella, E. Galli, J. D. Grice, F. Liebau, J. A. Mandarino, H. Minato, E. H. Nickel, E. Passaglia, D. R. Peacor, S. Quartieri, R. Rinaldi, M. Ross, R. A. Sheppard, E. Tillmanns, G. Vezzalini, *Can. Mineral.* **1997**, *35*, 1571.
- [10] A. Iijima, *Pure Appl. Chem.* **1980**, *52*, 2115.
- [11] R. L. Hay, *Studies in Surface Science and Catalysis*, Vol. 28, Elsevier Inc., Amsterdam, NL; Oxford, UK; Cambridge, US **1986**, 35.
- [12] C. Li, H. Zhong, S. Wang, J. Xue, Z. Zhang, *Colloids Surf. A Physicochem. Eng. Asp.* **2015**, *470*, 258.
- [13] A. Filippidis, *Hell. J. Geosci.* **2010**, *45*, 91.
- [14] K. Pavelić, M. Hadžija, L. Bedrica, J. Pavelić, I. Crossed, D. Signikić, M. Katić, M. Kralj, M. H. Bosnar, S. Kapitanović, M. Poljak-Blaži, Š. Križanac, R. Stojković, M. Jurin, B. Subotić, M. Čolić, *J. Mol. Med.* **2000**, *78*, 708.
- [15] P. Misaelides, *Microporous Mesoporous Mater.* **2011**, *144*, 15.
- [16] M. Moshoeshoe, M. Silas Nadiye-Tabbiruka, V. Obuseng, *Am. J. Mater. Sci.* **2017**, *2017*, 196.
- [17] J. Davidovits, *J. Thermal Anal.* **1991**, *37*, 1633.
- [18] A. Nikolov, I. Rostovsky, H. Nugteren, *Case Stud. Constr. Mater.* **2017**, *6*, 198.
- [19] G. Barone, M. C. Caggiani, A. Coccato, C. Finocchiaro, M. Fugazzotto, G. Lanzafame, R. Occhipinti, A. Stroschio, P. Mazzoleni, *IOP Conference Series: Materials Science and Engineering*, Vol. 777, Institute of Physics Publishing, Bristol, UK **2020**, 012001.
- [20] G. Barone, C. Finocchiaro, I. Lancellotti, C. Leonelli, P. Mazzoleni, C. Sgarlata, A. Stroschio, *Waste Biomass Valoriz.* **2021**, *12*, 1075. <https://doi.org/10.1007/s12649-020-01004-6>
- [21] C. Finocchiaro, G. Barone, P. Mazzoleni, C. Leonelli, A. Gharzouni, S. Rossignol, *Construct. Build Mater.* **2020**, *262*, 120095. <https://doi.org/10.1016/j.conbuildmat.2020.120095>
- [22] C. Finocchiaro, G. Barone, P. Mazzoleni, M. Sgarlata, C. Lancellotti, I. Leonelli, C. Romagnoli, *J. Mater. Sci.* **2021**, *56*, 513.
- [23] M. C. Caggiani, A. Coccato, G. Barone, C. Finocchiaro, M. Fugazzotto, G. Lanzafame, R. Occhipinti, A. Stroschio, P. Mazzoleni, *J. Raman Spectrosc.* **2021**. <https://doi.org/10.1002/jrs.6167>
- [24] R. Occhipinti, A. Stroschio, C. Finocchiaro, M. Fugazzotto, C. Leonelli, M. José Lo Faro, B. Megna, G. Barone, P. Mazzoleni, *Construct. Build Mater.* **2020**, *259*, 120391.
- [25] J. V. Smith, *Zeolites* **1984**, *4*, 309.
- [26] L. S. Campbell, J. Charnock, A. Dyer, S. Hillier, S. Chenery, F. Stoppa, C. M. B. Henderson, R. Walcott, M. Rumsey, *Mineral. Mag.* **2016**, *80*, 781.
- [27] E. Passaglia, *Am. Mineral.* **1970**, *55*, 1278.

- [28] E. Passaglia, G. Vezzalini, *Contrib. To Mineral. Petrol.* **1985**, 90, 190.
- [29] M. De'Gennaro, P. Cappelletti, A. Langella, A. Perrotta, C. Scarpato, *Contrib. To Mineral. Petrol.* **2000**, 139, 17.
- [30] B. M. Weckhuysen, J. Yu, *Chem. Soc. Rev.* **2015**, 44, 7022.
- [31] A. Alberti, D. Pongiluppi, M. G. Vezzalini, *NEUES Jahrb. FUR Mineral.* **1982**, 143, 231.
- [32] E. Galli, A. G. Loschi Ghittoni, *Am. Mineral.* **1972**, 57, 1125.
- [33] A. Alberti, G. Cruciani, I. Dauru, *Eur. J. Mineral.* **1995**, 7, 501.
- [34] W. Mozgawa, *J. Mol. Struct.* **2001**, 596, 129.
- [35] U. Barth-Wirsching, H. Holler, *Eur. J. Mineral.* **1989**, 1, 489.
- [36] R. J. M. Triana, R. J. F. Herrera, R. C. A. Rios, A. O. M. Castellanos, M. J. A. Henao, C. D. Williams, C. L. Roberts, *Earth Sci. Res. J.* **2012**, 16, 41.
- [37] M. E. Gunter, P. H. Ribbe, *Zeolites* **1993**, 13, 435.
- [38] J. D. Epping, B. F. Chmelka, *Curr. Opin. Colloid Interface Sci.* **2006**, 11, 81.
- [39] A. Bloise, C. B. Cannata, R. De Rosa, *Minerals* **2020**, 10, 3.
- [40] A. Langella, C. Colella, *Clays Clay Miner.* **1999**, 47, 348.
- [41] M. Ross, M. J. K. Flohr, D. R. Ross, *Am. Mineral.* **1992**, 77, 685.
- [42] H. van Koningsveld, J. M. Bennett, *Structures and Structure Determination*, Springer, Berlin, Germany **1999**, 1.
- [43] P. Vandenabeele, M. K. Donais, *Appl. Spectrosc.* **2016**, 70, 27.
- [44] J. Jehlička, P. Vandenabeele, H. G. M. Edwards, *Spectrochim. Acta - Part A Mol. Biomol. Spectrosc.* **2012**, 86, 341.
- [45] J. Jehlička, P. Vandenabeele, *J. Raman Spectrosc.* **2015**, 46, 927.
- [46] K. Eberhardt, C. Stiebing, C. Matthaüs, M. Schmitt, J. Popp, *Expert Rev. Mol. Diagn.* **2015**, 15, 773.
- [47] W. P. Griffith, *J. Chem. Soc. A Inorganic, Phys. Theor.* **1969**, 1372. <https://doi.org/10.1039/j19690001372>
- [48] B. Wopenka, J. J. Freeman, T. Nikischer, *Appl. Spectrosc.* **1998**, 52, 54.
- [49] G. Diego Gatta, V. Kahlenberg, R. Kaindl, N. Rotiroti, P. Cappelletti, M. De Gennaro, *Am. Mineral.* **2010**, 95, 495.
- [50] R. L. Frost, A. López, L. Wang, A. W. Romano, R. Scholz, *Spectrochim. Acta - Part a Mol. Biomol. Spectrosc.* **2015**, 137, 70.
- [51] P. P. Knops-Gerrits, D. E. De Vos, E. J. P. Feijen, P. A. Jacobs, *Microporous Mater.* **1997**, 8, 3.
- [52] Y.-L. Tsai, E. Huang, Y.-H. Li, H.-T. Hung, J.-H. Jiang, T.-C. Liu, J.-N. Fang, H.-F. Chen, *Minerals* **2021**, 11, 167.
- [53] C. I. Arkston, M. Gtinter, C. R. Knowles, *Can. Mineral.* **1993**, 31, 467.
- [54] P. S. R. Prasad, K. S. Prasad, *Microporous Mesoporous Mater.* **2007**, 100, 287.
- [55] P. Gillet, J. M. Malézieux, J. P. Itié, *Am. Mineral.* **1996**, 81, 651.
- [56] M. M. J. Treacy, J. B. Higgins, *Collection of simulated XRD powder patterns for zeolites*, 5th revised ed., Elsevier, Amsterdam, The Netherlands, Oxford, United Kingdom **2007**.
- [57] B. T. W. Lo, L. Ye, S. C. E. Tsang, *Chem* **2018**, 4, 1778.
- [58] A. Culka, J. Jehlička, *Anal. Chim. Acta.* **2021**, 339027. <https://doi.org/10.1016/j.aca.2021.339027>
- [59] C. L. Angell, *J. Phys. Chem.* **1973**, 77, 222.
- [60] P. K. Dutta, K. M. Rao, J. Y. Park, *J. Phys. Chem.* **1991**, 95, 6654.
- [61] D. Bersani, S. Andò, L. Scrocco, P. Gentile, E. Salvioli-Mariani, L. Fornasini, P. P. Lottici, *Minerals* **2019**, 9, 491.

## SUPPORTING INFORMATION

Additional supporting information may be found in the online version of the article at the publisher's website.

**How to cite this article:** C. Finocchiaro, A. Coccato, G. Barone, D. Bersani, A. Culka, L. Fornasini, P. Mazzoleni, J. Jehlička, A. Rousaki, P. Vandenabeele, *J Raman Spectrosc* **2022**, 53(3), 525. <https://doi.org/10.1002/jrs.6278>